PNAS
www.pnas.org

Supplementary Information for

Dark noise and retinal degeneration from D190N-rhodopsin

Daniel Silverman, Zuying Chai, Wendy W.S. Yue, Sravani Keerthi Ramisetty, Sowmya Bekshe Lokappa, Kazumi Sakai, Rikard Frederiksen, Parinaz Bina, Stephen Tsang, Takahiro Yamashita, Jeannie Chen, and King-Wai Yau

This PDF file includes:

www.pnas.org/cgi/doi/10.1073/pnas.2010417117

SUPPLEMENTARY TEXT

Confirmation of diminished D190N-Rho content in *Rho*$^{D190N/REY}$ rods.

From the probability-of-failure experiment in Fig. 2, we estimated that the functional pigment content in *Rho*$^{D190N/REY}$*;Gcaps*$^{-/-}$ rods was (4.8 ± 1.3) × 10^6 D190N-Rho molecules rod^{-1}, which was significantly lower than the WT-Rho content in *Rho*$^{WT/WT}$*;Gcaps*$^{-/-}$ rods (Fig. 2C). Similarly, based on physiological action spectra in *Rho*$^{D190N/REY}$ rods, we estimated the D190N-Rho content was (6.2 ± 4.4) × 10^6 D190N-Rho molecules rod^{-1} (*SI Appendix*, Fig. S1A and legend). To determine the relative amounts of D190N-Rho and REY-Rho in the *Rho*$^{D190N/REY}$ retina, we performed isoelectric focusing (1, 2) with *Rho*$^{D190N/REY}$ retinae. This method separated D190N-Rho and REY-Rho according to their distinct isoelectric points (Supplementary Fig. S1B). *Rho*$^{D190N/REY}$ consisted of ~33% ± 8% D190N-Rho and ~67% ± 8% REY-Rho molecules (n = 4 retinae), supporting the conclusion that D190N-Rho content was diminished.

From spectrophotometry with whole-retina extracts we found that the total pigment content in the *Rho*$^{D190N/REY}$ retina was 0.06 ± 0.02 nmol retina^{-1} (n = 4 retinae from 1- to 2-month old animals, based on single-wavelength 500-nm absorption), or ~80% lower than the normal pigment content in the *Rho*$^{WT/WT}$ retina. This was an even larger drop than the ~40% reduction in total pigment content in *Rho*$^{D190N/REY}$ rods measured from microspectrophotometry (Fig. 2D). A likely explanation is that the microspectrophotometry measurements targeted rods with relatively long outer segments as opposed to rods with shortened or missing outer segments, whereas whole-retina

spectrophotometry covers all rods across the retina. Taken together, all results point to D190N-Rho content being substantially reduced.

SUPPLEMENTARY METHODS

Animals

All animal experiments were conducted according to protocols approved by the Institutional Animal Care and Use Committee at Johns Hopkins University. Mice were raised under 14/10-hr light/dark cycle, and an animal was dark-adapted overnight before suction-pipette recording experiments. Both male and female mice at 1-3 months old were used for experiments.

Suction-Pipette Recording

Single-cell recordings were performed as described previously (3). Briefly, after overnight dark adaptation and euthanasia, eyes were removed under dim red light and retinae isolated under infrared illumination in Locke's solution, containing 112.5-mM NaCl, 3.6-mM KCl, 2.4-mM $MgCl_2$, 1.2-mM $CaCl_2$, 3-mM Na_2-succinate, 0.5-mM Na-glutamate, 0.02-mM EDTA, 10-mM glucose, 0.1%-MEM vitamins (M6895, Sigma-Aldrich), 0.1%-MEM amino-acid supplement (M5550, Sigma-Aldrich), 10-mM HEPES, pH 7.4 and 20-mM $NaHCO_3$. Retinae were stored at room temperature in Locke's solution bubbled with 95% O_2/5% CO_2, to be used for experiments within 6 hrs of isolation.

Before recording, a piece of the retina was chopped into small fragments with a razorblade in Lock's solution on a Sylgard-coated petri dish (24236-10; Electron

Microscopy Sciences). Recording chamber was perfused with Locke's solution at 37 °C. Temperature was monitored by a thermistor held within several millimeters of the recorded cell. Suction-pipette recording was carried out from individual rods under infrared light using a tight-fitting glass pipette containing 140-mM NaCl, 3.6-mM KCl, 2.4-mM $MgCl_2$, 1.2-mM $CaCl_2$, 0.02-mM EDTA, 10-mM glucose and 3-mM HEPES, pH 7.4. The pipette resistance was ideally ~7-8 MΩ in recording solutions without a cell drawn in.

Stimulation flashes were 10-ms in duration and typically of 500-nm light except for action-spectra experiments. The effect of temperature on action spectra was evaluated by comparing cohorts of cells studied at 37°C or 25°C. Responses and dark noise were primarily low-pass filtered at 1 kHz and sampled at 2 kHz with an Axopatch 200B amplifier. Two additional channels were low-pass filtered at 20 Hz and 3 Hz (RC filter, Krohn-Hite 3343). The 1-kHz channel was compared with the 20- or 3-Hz channels in order to correct the time delay caused by filtering. Dark noise recordings were plotted at 3 Hz and flash responses at 20 Hz.

Evaluating retinal morphology using histological cross sections

Histology was as described previously (4). Briefly, the eye was marked at the superior pole for orientation, then punctured and fixed overnight at 4°C in ½ Karnovsky Buffer (2.5%-glutaraldehyde, 2.0%-formaldehyde in 0.1-M cacodylate solution, pH 7.2). Fixed eyes were stored in 0.1-M cacodylate solution, pH 7.2 until further processed for sectioning. Lenses were removed and fixed eyecups were further fixed with 1%-osmium tetraoxide in 0.1-M cacodylate buffer for 1.5–2.0 hrs at room temperature. Eyecups were washed 2 × 10 min with 0.1-M cacodylate buffer, pH 7.2 and dehydrated (15 min each with 50%-, 70%-, 85%-, and 95%-ethanol; 3 × 10 min 100%-ethanol; and 2 × 10 min 100%

propylene oxide). Infiltration with epon (25% w/w epon 812, 15% w/w Araldite 502, 55% w/w DDSA, 4% w/w DBP, and 3% -BDMA) was performed by overnight incubation with 1:1 epon:propylene oxide followed by overnight incubation with 2:1epon:propylene oxide and then 6-hr to overnight incubation with 100%-epon. The eyecups were placed in molds filled with epon with the optic nerve in back and the superior pole pointing at 12 o'clock. Samples were baked for 3–4 days at 55°C. After hardening, epon-embedded eyes were cut into 1-μm sections and stained with Richardson stain (0.5% methylene blue, 0.5% Azine II, and 0.5% borax in dH2O). Sections were scanned using Aperio Image Scope and measurements of outer-nuclear-layer thickness and outer-segment length were made in ten equal distance regions across the superior-inferior axis of the retina.

Dye labeling of misfolded-protein aggregates using retinal cryosections

Following transcardial perfusion, an isolated eyeball was punctured with a 25-gauge needle and fixed overnight at 4ºC with 4% PFA in phosphate-buffered saline. The cornea and lens were removed and the eyecup was dehydrated in 15% sucrose for 12-24 hours followed by further dehydration in 30% sucrose for 12-24 hours. The eyecup was then embedded in Optimal Cutting Temperature (OCT, Tissue-Tek) and rapidly frozen in 2-methylbutane chilled in a beaker surrounded by crushed dry ice. Retinal sections of 15-μm thickness were air dried and slides were processed for staining with PROTEOSTAT (Enzo Life Sciences, ENZ-51035-0025) according to the manufacturer's instructions. Briefly, sections were rinsed with PBS, permeabilized in 0.5% Triton X-100, 3 mm EDTA, pH 8.0, and stained for 30 minutes at room temperature in a solution containing PROTEOSTAT and Hoechst 33342 nuclear stain. Slides were rinsed with PBS, mounted

with Aqua-Poly/Mount (Polysciences, 18606-20) and imaged using a confocal microscope (Zeiss, LSM 880).

Measuring chromophore exchange with spectrophotometry

Visual pigments were purified as described previously (5). Bovine WT-Rho, bovine D190N-Rho, and chicken M-cone pigment were transiently expressed in HEK293S cells. The cDNA of chicken M-cone pigment was tagged at the C terminus with Rho-1D4 sequence (ETSQVAPA). Mammalian expression vectors pUSRα or pCAGGS containing cDNA for each pigment were transfected and cells were collected by centrifugation and suspended in Buffer A (50-mM HEPES, 140-mM NaCl, pH 6.5), and 11-*cis*-retinal was added to the cell suspension to regenerate pigments. Cells were solubilized with Buffer A containing 1%-dodecyl maltoside (DDM) and adsorbed to a Rho1D4 affinity column. After washing with Buffer A containing 0.02%-DDM, the recombinant pigments were eluted by addition of the synthetic peptide corresponding to the epitope sequence. To assess chromophore exchange, 9-*cis*-retinal was applied to each purified dark-state pigment and difference spectra were calculated after the durations indicated in figure legend. Maximally blue-shifted spectra were determined by fully regenerating each pigment with 9-*cis*-retinal.

Evaluating photon capture and apo-opsin content in intact mouse rods using microspectrophotometry

Microspectrophotometry was as described previously (6, 7). The retina was isolated in HEPES (10-mM, pH 7.4)-buffered Ames medium (A1420, Sigma-Aldrich) under infrared illumination. A piece of retina was transferred to a 2-mm-deep Plexiglass

recording chamber, gently flattened by forceps on the bottom quartz cover-slip window of the chamber with the photoreceptors facing the incident light, and then secured by a slice anchor (Warner Instruments). The recording chamber was placed on a microscope stage located in the beam path of a custom-built microspectrophotometer. Perfusion in the chamber was at 4 ml/min with 35–37°C Ames medium (Sigma-Aldrich) buffered with sodium bicarbonate and equilibrated with 95%-O_2 + 5%-CO_2. Absorption spectra were measured at the edge of the retinal piece where outer segments could be seen projecting transversely across the incident light beam. In this way, the polarization of the incident beam was parallel to the plane of the intracellular disks (T-polarization). Measurements were taken over the wavelength range of 300 – 700 nm with a 2-nm resolution. Optical density was calculated from Beers' Law, OD = $\log(I_i/I_t)$, where I_i is light transmitted through a tissue-free space close to the outer segments, and I_t is the light transmitted through intact outer segments. To search for any sign of excess apo-opsin, we applied 50-μM 11-*cis*-retinal to dark-adapted tissue for 15 minutes and measured the optical density. Any increase in optical density at the spectral peak of rhodopsin would indicate that new pigment had been formed by excess apo-opsin (6).

Isoelectric focusing to quantify the relative amounts of distinct rhodopsin species

All mice were dark-adapted and retinae were isolated under infrared light. Tissues were frozen in liquid N_2, and kept in -80ºC until further processing. Isoelectric focusing was performed as described in (1). Briefly, samples were homogenized in buffer (25-mM HEPES pH 7.5,100-mM EDTA, 50-mM NaF, 5-mM adenosine). Membrane was pelleted by centrifugation (13,000 × g) for 15 min, washed in 10-mM HEPES (pH 7.5) and resuspended in buffer (10-mM HEPES pH 7.5, 1-mM $MgCl_2$, 0.1-mM EDTA, 2% BSA,

50-mM NaF, 5-mM adenosine) with 3-fold molar excess of 11-*cis*-retinal and incubated overnight at 4ºC. On the next day, the membrane was pelleted and washed, and solubilized in buffer (10-mM HEPES, pH 7.5, 1-mM $MgCl_2$, 0.1-mM EDTA, 1%-dodecyl-maltoside, 1-mM DTT). A flat-bed acrylamide gel was made, with a pH gradient formed with 3.8%-Pharmalyte pH 2.5-5 and 2.5% Pharmalyte 5-8 (SigmaAldrich). The anode solution was 0.04-M glutamic acid, and the cathode solution was 1-M NaOH. The gel was pre-focused for 30 min at 23 W constant power. The samples were placed on the gel and focused for 2 hrs at the same power. The gel was blotted onto nitrocellulose, and rhodopsin was detected using 4D2 (8), a mouse monoclonal antibody against the N-terminus of rhodopsin.

Western blots for components of the unfolded protein response

Retinae were dissected under room light. Each retina was homogenized in 150 µl buffer (150-mM NaCl, 50-mM Tris, pH 8.0, 0.1% Nonidet P-40, 0.5% deoxycholic acid) containing 0.1-mM PMSF, complete mini protease inhibitor (Roche Applied Sciences), and 50-µM NaF. Protein concentration of each sample was determined by the BCA protein assay kit (ThermoFisher Scientific). Equal amount from each sample was electrophoresed on 4–12% Bis-Tris SDS-PAGE gel (Invitrogen) followed by transfer to nitrocellulose membrane (WhatmanTM; GE Healthcare Life Sciences) and incubated overnight with the following primary antibodies: rabbit anti-ATF3 (1:1,000, SigmaAldrich, HPA001562), rabbit anti-ATF4 (1:1,000, ThermoFisher Scientific PA5-27576) and mouse anti-actin (1:5,000, Millipore, MAB1501). Membrane was then incubated with fluorescently-labeled secondary antibodies (1:10,000, LI-COR biosciences) and detected using the Odyssey infrared imaging system and signals were quantified using the Odyssey system and ImageJ (Fiji).

Quantification and Statistical Analysis

All values presented are Mean ± S.D., unless specified. Data was analyzed using custom MATLAB scripts. Number of cells were determined based on the variation of the measurement and are provided in the text and legends. For physiological recordings, data with obvious changes in cell state during recording (e.g. abrupt shift in dark current from mechanical damage caused by the pipette) were excluded from analyses. Unless otherwise specified, for quantitative conclusions, reported *p*-values are from Student's *t*-test.

Data Availability

All data and analysis code will be made available from the corresponding author upon reasonable request.

Supplementary References

1. Lokappa S, Cornwall M, Chen J (2019) Isoelectric focusing to quantify rhodopsin phosphorylation in mouse retina. *BIO-PROTOCOL* 9(14). doi:10.21769/bioprotoc.3300.
2. Berry J, et al. (2016) Effect of rhodopsin phosphorylation on dark adaptation in mouse rods. *J Neurosci* 36(26):6973–6987.
3. Yue WWS, et al. (2019) Elementary response triggered by transducin in retinal rods. *Proc Natl Acad Sci* 116(11):5144–5153.
4. Wang T, Chen J (2014) Induction of the unfolded protein response by constitutive

G-protein signaling in rod photoreceptor cells. *J Biol Chem* 289(42):29310–29321.

5. Kojima K, Imamoto Y, Maeda R, Yamashita T, Shichida Y (2014) Rod visual pigment optimizes cctive state to achieve efficient G-protein activation as compared with cone visual pigments. *J Biol Chem* 289(8):5061–5073.
6. Nymark S, Frederiksen R, Woodruff ML, Cornwall MC, Fain GL (2012) Bleaching of mouse rods: microspectrophotometry and suction-electrode recording. *J Physiol* 590(10):2353–2364.
7. Frederiksen R, et al. (2012) Low aqueous solubility of 11-cis-retinal limits the rate of pigment formation and dark adaptation in salamander rods. *J Gen Physiol* 139(6):493–505.
8. Hicks D, Molday RS (1986) Differential immunogold-dextran labeling of bovine and frog rod and cone cells using monoclonal antibodies against bovine rhodopsin. *Ezp Eye Res* 42:55–71.
9. Liu MY, et al. (2013) Thermal stability of rhodopsin and progression of retinitis pigmentosa: comparison of S186W and D190N rhodopsin mutants. *J Biol Chem* 288(24):17698–17712.

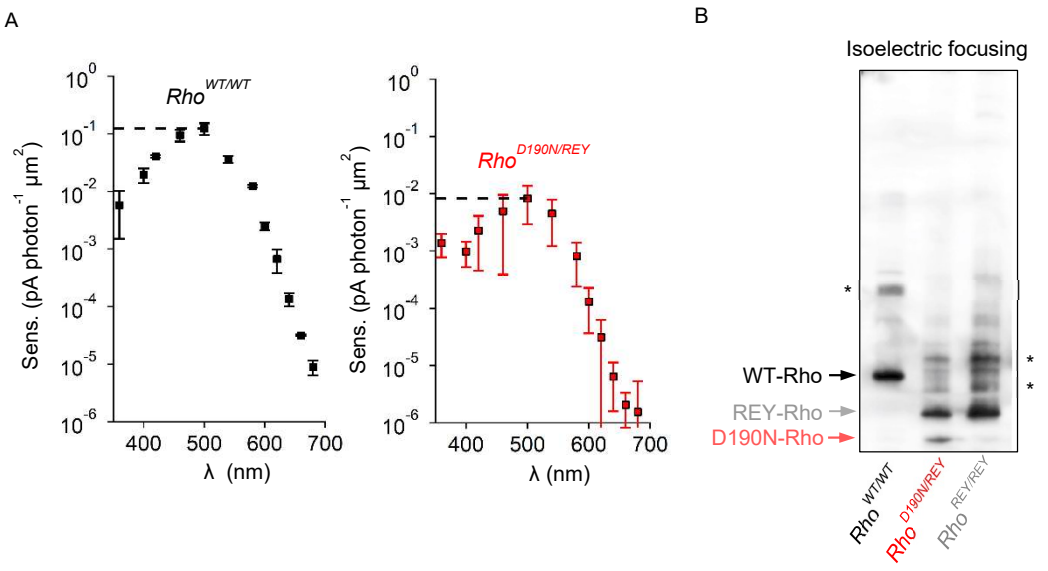

Fig. S1. D190N-Rho content is diminished in *Rho*$^{D190N/REY}$ rods compared to WT-Rho in *Rho*$^{WT/WT}$ rods. (*A*) Physiological action spectra for *Rho*$^{WT/WT}$;*Gcaps*$^{+/+}$ and *Rho*$^{D190N/REY}$;*Gcaps*$^{+/+}$ rods. Fractional pigment content was estimated by taking the ratio of peak sensitivities (dashed lines) after adjusting for D190N-Rho's 6%-smaller extinction coefficient (9), [(0.008/0.94) / 0.123 = 0.07]. Thus, based on these action spectra, the D109N-Rho content was estimated to be 0.07 × (8.8 × 10^7) = (6.2 × 10^6) D190N-Rho molecules rod^{-1}. (*B*) Isoelectric focusing (*SI Appendix*, Supplementary Methods) blot showing WT-Rho in *Rho*$^{WT/WT}$, D190N-Rho and REY-Rho in *Rho*$^{D190N/REY}$, and REY-Rho in the *Rho*$^{REY/REY}$ sample. Stars mark bands that appeared to result from rhodopsin's interaction with impurities in a specific batch of dodecyl-maltoside, which were not present in some experiments (see Fig. 3F). This method separated D190N-Rho and REY-Rho according to their distinct isoelectric points, demonstrating that the pigment content in *Rho*$^{D190N/REY}$ consisted of ~33% ± 8% D190N-Rho and ~67% ± 8% REY-Rho molecules (n = 4 retinae).

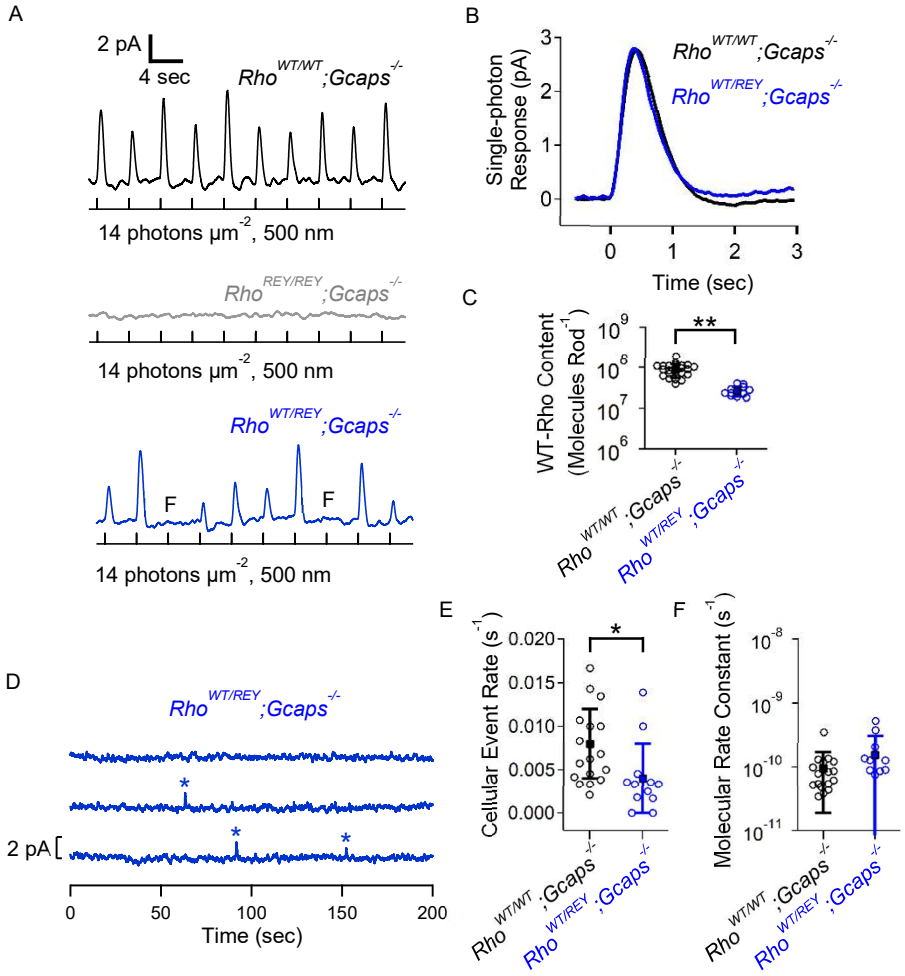

Fig. S2. WT-Rho content and spontaneous activity in *Rho$^{WT/REY}$;Gcaps$^{-/-}$* rods. *(A)* Repeated dim flashes on *Rho$^{WT/WT}$;Gcaps$^{-/-}$* rods (black), *Rho$^{REY/REY}$;Gcaps$^{-/-}$* rods (gray), and *Rho$^{WT/REY}$;Gcaps$^{-/-}$* (blue, response failures marked by "F"). *(B)* Single-photon responses from WT-Rho were very similar in *Rho$^{WT/WT}$;Gcaps$^{-/-}$* and in *Rho$^{WT/REY}$;Gcaps$^{-/-}$* rods. This similarity, as found also between *Rho$^{WT/WT}$;Gcaps$^{-/-}$* and in *Rho$^{D190N/REY}$;Gcaps$^{-/-}$* rods (see Fig. 2B), supports the proposal that the Ca^{2+}-mediated negative feedback underlies the faster response decline in *Rho$^{WT/REY}$* rods. *(C)* Functional rhodopsin content based on the measured probability of failure (Methods). The WT-Rho content in *Rho$^{WT/REY}$;Gcaps$^{-/-}$* rods was $(2.6 \pm 0.7) \times 10^7$ molecules rod^{-1} compared to $(8.8 \pm 3.4) \times 10^7$

WT-Rho molecules in $Rho^{WT/WT};Gcaps^{-/-}$ rods. Double star marks statistical significance of $p < 0.0001$. *(D)* Dark noise from WT-Rho in $Rho^{WT/REY};Gcaps^{-/-}$. *(E)* Cellular rate of spontaneous-isomerization events in $Rho^{WT/WT};Gcaps^{-/-}$ and $Rho^{WT/REY};Gcaps^{-/-}$ rods. Single star marks statistical significance of $0.0001 \leq p \leq 0.05$. *(F)* Molecular rate constant of spontaneous isomerization for WT-Rho in $Rho^{WT/WT};Gcaps^{-/-}$ ($\sim 9.1 \times 10^{-11}$ s^{-1}) and in $Rho^{WT/REY};Gcaps^{-/-}$ rods ($\sim 1.5 \times 10^{-10}$ sec^{-1}). There was not a significant difference between the two genotypes.

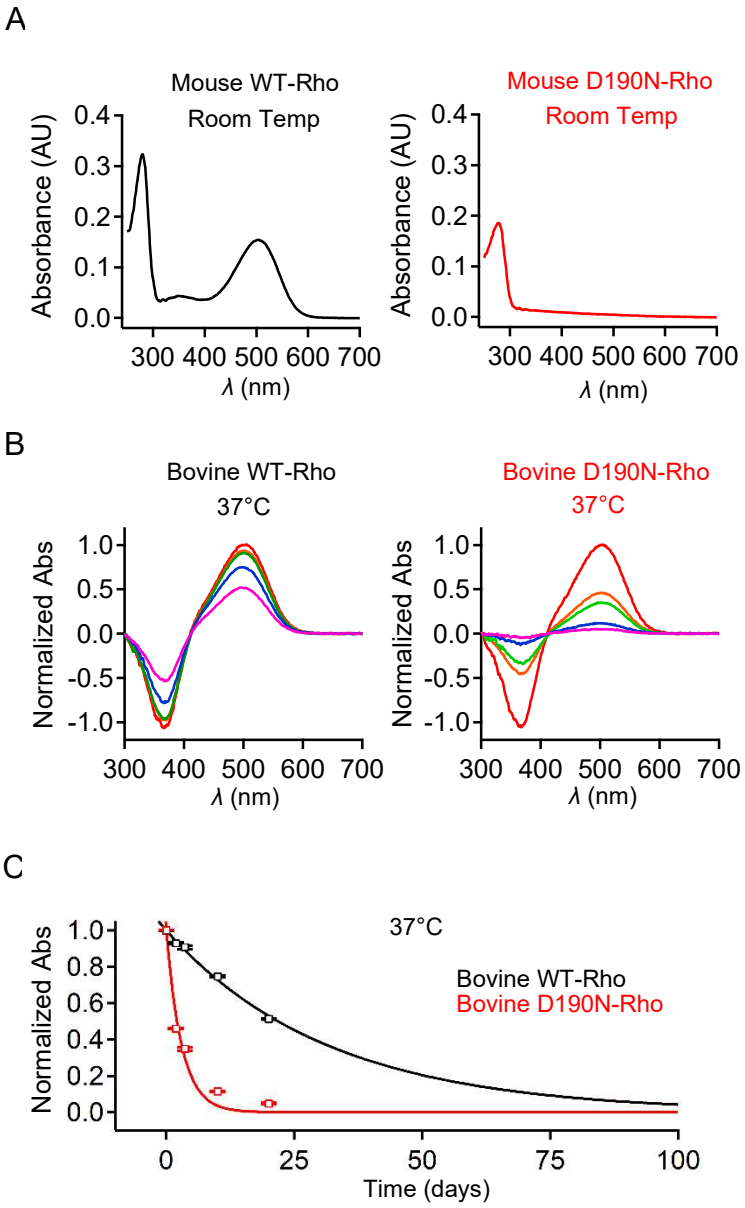

Fig. S3. Instability of D190N-Rho versus WT-Rho *in vitro*. (*A*) Spectrophotometry with HEK293 cell extracts after transfection of mouse WT-Rho (left) and mouse D190N-Rho (right). Mouse D190N-Rho could not be reconstituted with chromophore in vitro. (*B*) Spectrophotometry with HEK293 cell extracts after transfection of bovine WT-Rho (left) and bovine D190N-Rho (right). (*C*) Time course of the disappearance of bovine WT-Rho

and D190N-Rho absorbance spectra at 37°C. Data points were fit by single-exponential decay functions with τ = 31.5 days for WT-Rho and τ = 3 days for D190N-Rho. Bovine D190N-Rho decayed at a rate ~10.5-fold faster than WT-Rho. Such *in vitro* decay consists of spontaneous isomerization, spontaneous release of 11-*cis*-retinal, and unfolding of rhodopsin (9).

Table S1A. Flash response paramaters of mouse rods for evaluating effects of D190N-Rho in *Gcaps*$^{+/+}$ rods

Genotype	ROS length (μm)	I_{Dark} (pA)	S_F (pA photon^{-1} μm^2)	a (pA)	t_{int} (ms)	t_{peak} (ms)	τ_{rec} (ms)
(1) *Rho*$^{WT/WT}$	18.5 ± 2.6 (n = 48)	15.9 ± 2.0 (n = 9)	0.280 ± 0.090 (n = 9)	0.64 ± 0.15 (n = 9)	371 ± 79 (n = 9)	136 ± 12 (n = 9)	249 ± 70 (n = 9)
(2) *Rho*$^{WT/REY}$	16.4 ± 4.0* (n = 25)	13.9 ± 0.7* (n = 8)	0.072 ± 0.022** (n = 9)	0.61 ± 0.17 (n = 9)	280 ± 44* (n = 9)	128 ± 15 (n = 15)	203 ± 38 (n = 9)
(3) *Rho*$^{D190N/WT}$	11.7 ± 2.4** (n = 30)	12.9 ± 2.1* (n = 13)	0.070 ± 0.021** (n = 13)	-	-	-	-
(4) *Rho*$^{D190N/REY}$	11.8 ± 2.0** (n = 21)	15.4 ± 3.5 (n = 26)	0.008 ± 0.004** (n = 12)	0.53 ± 0.37 (n = 12)	232 ± 126* (n = 12)	129 ± 20 (n = 12)	132 ± 63* (n = 12)

Table S1B. Flash response paramaters of mouse rods for evaluating effects of D190N-Rho in *Gcaps*$^{-/-}$ rods

Genotype	ROS length (μm)	I_{Dark} (pA)	S_F (pA photon^{-1} μm^2)	a (pA)	t_{int} (ms)	t_{peak} (ms)	τ_{rec} (ms)
(1) *Rho*$^{WT/WT}$;*Gcaps*$^{-/-}$	18.0 ± 1.2^{+} (n = 29)	14.8 ± 1.6^{+} (n = 10)	1.26 ± 0.46 (n = 23)	2.9 ± 1.5 (n = 23)	629 ± 92 (n = 23)	403 ± 42 (n = 23)	230 ± 86 (n = 23)
(2) *Rho*$^{WT/REY}$;*Gcaps*$^{-/-}$	13.2 ± 2.5** (n = 40)	13.4 ± 3.5 (n = 15)	0.35 ± 0.08** (n = 13)	2.9 ± 0.6 (n = 13)	624 ± 141 (n = 13)	382 ± 55 (n = 13)	299 ± 137 (n = 13)
(3) *Rho*$^{D190N/WT}$;*Gcaps*$^{-/-}$	8.5 ± 1.2** (n = 32)	8.32 ± 2.0** (n = 16)	0.42 ± 0.22** (n = 16)	-	-	-	-
(4) *Rho*$^{D190N/REY}$;*Gcaps*$^{-/-}$	12.0 ± 2.0** (n = 21)	13.7 ± 1.7 (n = 12)	0.05 ± 0.02** (n = 12)	2.8 ± 0.8 (n = 12)	625 ± 69 (n = 12)	414 ± 40 (n = 12)	319 ± 132* (n = 12)

Values are mean ± SD, with the number of cells analyzed (n) in parentheses. $^{+}$Values from [Ref. (3)]. Rod outer segment (ROS) length is the approximate length of live rod outer segments measured with light microscopy. Flash responses were measured from calibrated 10-ms flashes of 500-nm light. I_{Dark} is the maximum response amplitude representing the dark current; S_F is the flash sensitivity; a is the single-photon response amplitude; t_{int} and t_{peak} are the integration time and time-to-peak of dim-flash responses, respectively; τ_{rec} is the recovery time constant obtained from exponential fits to the final decay of dim-flash responses (*Methods*). Single stars mark statistical significance of $0.0001 \leq p \leq 0.05$ and double stars mark $p < 0.0001$, from Student's t-tests comparing each genotype [(2), (3), (4)] to the *Rho*$^{WT/WT}$ control (1).